

Cardiomyopathy in zebrafish due to mutation in an alternatively spliced exon of *titin*

Xiaolei Xu^{1*}, Steffen E. Meiler^{1*}, Tao P. Zhong¹, Manzoor Mohideen¹, Dane A. Crossley², Warren W. Burggren³ & Mark C. Fishman¹

*These authors contributed equally to this work.

Published online: 14 January 2002, DOI: 10.1038/ng816

The zebrafish embryo is transparent and can tolerate absence of blood flow because its oxygen is delivered by diffusion rather than by the cardiovascular system¹. It is therefore possible to attribute cardiac failure directly to particular genes by ruling out the possibility that it is due to a secondary effect of hypoxia. We focus here on *pickwick*^{m171} (*pik*^{m171}), a recessive lethal mutation discovered in a large-scale genetic screen². There are three other alleles in the *pik* complementation group with this phenotype (*pik*^{m242}, *pik*^{m740}, *pik*^{m186}; ref. 3) and one allele (*pik*^{mV062H}) with additional skeletal paralysis⁴. The *pik* heart develops normally but is poorly contractile from the first beat. Aside from the edema that inevitably accompanies cardiac dysfunction, development is normal during the first three days. We show by positional cloning that the 'causative' mutation is in an alternatively-spliced exon of the gene (*ttn*) encoding Titin. Titin is the biggest known protein and spans the half-sarcomere from Z-disc to M-line in heart and skeletal muscle⁵. It has been proposed to provide a scaffold for the assembly of thick and thin filaments⁶ and to provide elastic recoil engendered by stretch during diastole⁷. We found that

nascent myofibrils form in *pik* mutants, but normal sarcomeres are absent. Mutant cells transplanted to wildtype hearts remain thin and bulge outwards as individual cell aneurysms without affecting nearby wildtype cardiomyocytes, indicating that the contractile deficiency is cell-autonomous. Absence of Titin function thus results in blockage of sarcomere assembly and causes a functional disorder resembling human dilated cardiomyopathies, one form of which is described in another paper in this issue⁸. We mapped *pik* to a 1.2-cM region of LG9 using microsatellite markers. 'Walking' with YACs and BACs (Fig. 1) revealed the critical interval overlapping the *ttn* genomic region. As the recombinants on the Z8363 (telomeric) side were outside of *ttn* and vertebrate *ttn* cDNA is over 80 kb in other species⁵, complete sequence analysis was impractical. Because *titin* is expressed in both skeletal and cardiac muscle without detectable skeletal muscle abnormality in the four cardiac-specific alleles, we speculated that the mutation might be within exons spliced in a cardiac-specific manner. In human and rat, cardiac *titin* mRNA differs from skeletal isoforms in that it always contains an N2B sequence (Fig. 2a)⁹. We therefore cloned the

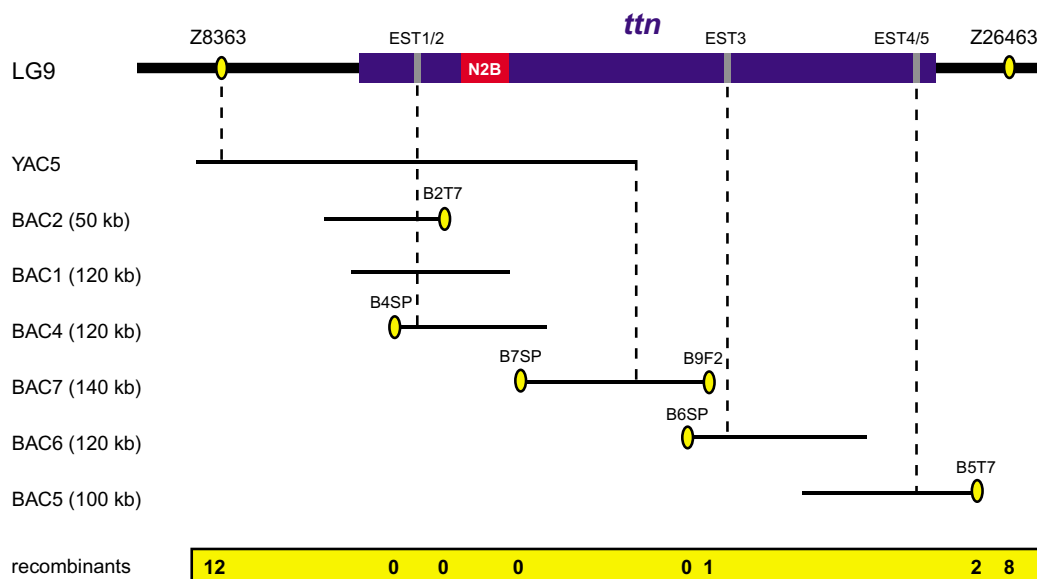


Fig. 1 Positional cloning of the *pik* locus. The walk for *pik* was initiated from SSLP marker Z8363, and the *ttn* genomic region was covered with BACs. SSCP markers are represented by yellow ovals and the number of recombinants are summarized at the bottom. Recombinants are from 1,862 meioses. EST1–5 corresponds to: A1588514, A1588106, A1601282, A1353993 and A1629069, respectively.

¹Cardiovascular Research Center, Massachusetts General Hospital, 149 13th Street, Charlestown, Massachusetts 02129, USA. ²Department of Biological Sciences, University of California at Irvine, Irvine, California 92697, USA. ³Department of Biological Sciences, University of North Texas, Denton, Texas 76203, USA. Correspondence should be addressed to M.C.F. (e-mail: fishman@cvc.harvard.edu).

exon encoding the zebrafish N2B domain. This domain is expressed in the heart but not in skeletal muscle (Fig. 2c). We found a T→G transversion consistently in the N2B exon of *pik^{m171}* mutants (Fig. 2b,d). The mutation is located in the unique sequence (IS3 domain; Fig. 2a) within the cardiac-specific N2B exon.

To confirm that the mutation in *ttn* causes the phenotype, we injected morpholino antisense oligonucleotides into the embryos at the 1–4-cell stage. To examine specifically the effects of perturbations of the N2B-containing transcript, we designed an oligonucleotide (MO1) to target the splice donor site at the 3' end of the N2B-containing exon. Targeting morpholinos to splice donor sites has been shown previously to disrupt gene function by perturbing the targeted splicing event¹⁰. Semi-quantitative RT-PCR (Fig. 2e) indicates that MO1 disrupts the N2B site (revealed by primer set 1) but not the skeletal muscle-specific exon (primer set 2) or the constitutively spliced region (primer set 3). A morpholino targeted to a skeletal muscle-specific splice donor (MO2) perturbs that region (primer set 2) but not N2B (primer set 1). The injection of MO1, the morpholino directed to the cardiac-specific N2B splice donor, results in an exact phenotype of the *pik^{m171}* allele. Cardiac contractility is reduced, but skeletal muscle seems to be normal. The cardiac effect is dose-dependent but potent, and is seen in 100% of embryos injected with as little as 10 ng (Fig. 2f). Injection of the morpholino designed to interfere with the skeletal muscle-specific splice donor perturbs somite structure and causes near paralysis but does not affect cardiac development or function.

At the organ level, the consequence of the mutation seems to be reduction in systolic pressure, because there is little if any blood ejected and the dilated heart empties only little during systole. Using microangiography¹¹, however, we could not visualize downstream vessels (data not shown).

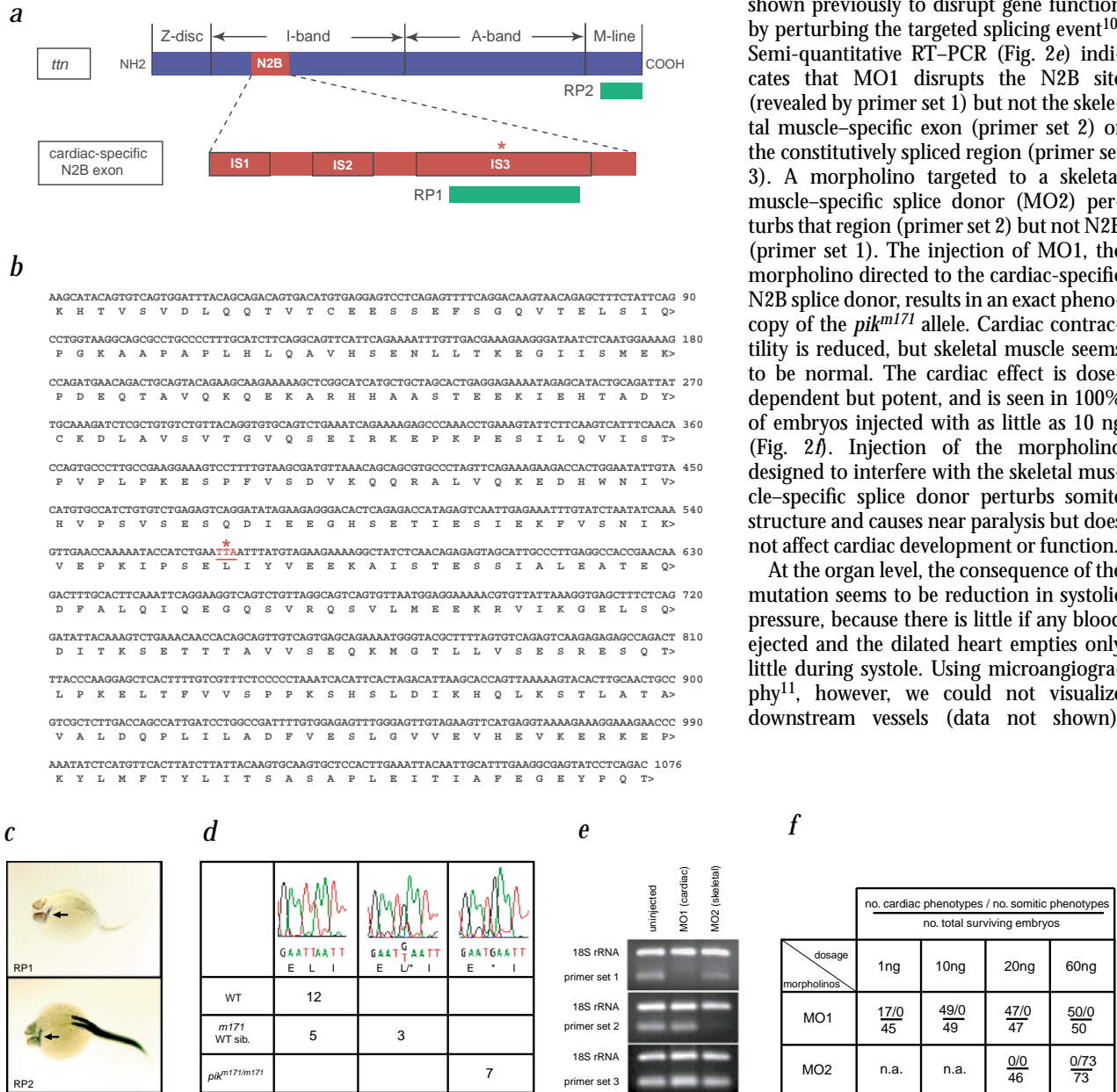
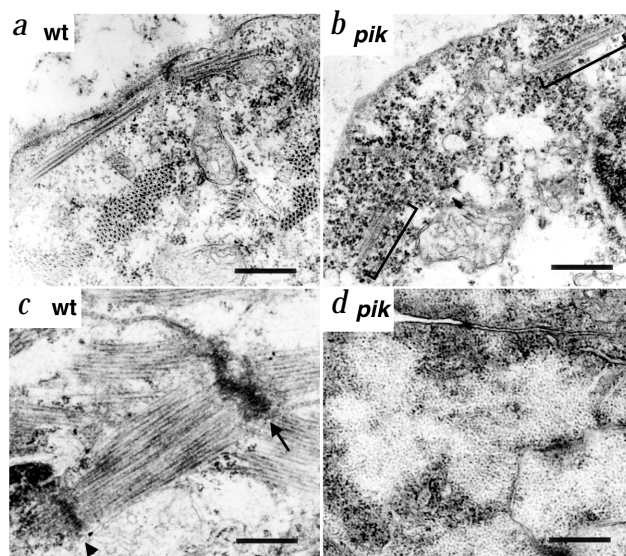


Fig. 2 *ttn* is the *pickwick* gene. **a**, Modular structure of *ttn*. Vertebrate Titin has a molecular mass of 3,000 kD, of which 90% are repeats of immunoglobulin C2 (Ig) domains and fibronectin type III (FN3) domains⁵. The amino terminus is at the Z-disc, and the carboxy terminus at the M-line. The N2B exon is located within the I-band region. As does human *TTN*, the N2B exon from zebrafish contains three unique sequences (IS1, IS2 and IS3). The asterisk shows the position of the nonsense mutation identified in the *pik^{m171}* allele. Green bars indicate the positions of RP1 and RP2, two riboprobes used for *in situ* whole-mount staining. **b**, Sequence of the RP1 riboprobe within the IS3 domain and the deduced peptides. The position of the nonsense mutation is marked by an asterisk, and the affected codon is underlined. **c**, N2B is a cardiac-specific domain in zebrafish. A dorsal-lateral view of 1-dpf embryos after *in situ* hybridization is shown. Riboprobe RP1, derived from the N2B exon, stains heart only. Riboprobe RP2, derived from the end of the *ttn* cDNA, labels both somites and heart. Arrows indicate the staining of the heart. **d**, A T→G transversion is identified in *pik^{m171}*. This would change a leucine to a stop codon. This transversion was first detected in the cDNA isolated by RT-PCR from the *pik^{m171/m171}* embryos, and later confirmed in genomic sequences from seven homozygous *pik^{m171/m171}* embryos. Of the eight wildtype siblings, three show a mixture of T/G at the position, indicating they are heterozygous at the locus. **e**, Morpholinos against splice donor sites disrupt the targeted splicing events. Morpholino MO1 was designed to target the splice donor site of the cardiac-specific N2B exon. Morpholino MO2 was designed to target the splice donor site of the I79 domain (which is skeletal muscle-specific in other species¹⁰). Primer sets 1 and 2 are primer pairs that amplify the end products of the targeted splicing events, involving N2B and I79 respectively. Primer set 3 is a primer pair that monitors constitutive splicing between exon 111 and 112. Exons are named using the human terminology¹⁰, based on homology and position. **f**, The cardiac-specific phenotype of *pik* is phenocopied by injection of MO1 in a dose-dependent manner. In contrast, injection of MO2 does not disturb cardiac contractility, but instead disrupts somite development, causing a near-paralysis of the embryos.

Fig. 3 Sarcomeric structures are disrupted in *pik* mutant embryos. Transverse sections of ventricle cells are shown by transmission electron microscopy. **a**, In wildtype hearts at 36 hpf, there are nascent myofibrils. **b**, In *pik*^{m171/m171} mutant embryos, the amounts of myofibrils are significantly reduced. Thick and thin elements do assemble, but only in small patches (brackets). **c**, In wildtype embryos at 48 hpf, nascent myofibrils assemble into higher-order sarcomere structures. An example of a sarcomere between a Z-disc (arrowhead) and an intercalated disc (arrow) is shown. **d**, In *pik*^{m171/m171} embryos at 48 hpf, no myofibrils could be detected. Scale bars=0.5 μ m.



Thus, we could not be certain whether poor systolic emptying was due to vascular obstruction with consequent high afterload or to a primary defect in contractility. We directly assayed pressure in the ventricle by the null balance feedback system¹². We found that the ventricular pressure in *pik* mutants is markedly less than that in the wild type (0.084 \pm 0.008 versus 0.49 \pm 0.06 mm Hg). The *pik* heart thus generates little systolic force.

The cells of the *pik* mutant are thin but do contract. This is notable, as it has been speculated that Titin is essential for sarcomere assembly³. In particular, Titin is believed to form the scaffold needed to align the thick and thin filaments in proper register and at correct interfilament distance¹³. We therefore examined the sarcomeric structure of the cardiac myocytes by transmission electron microscopy. In the cardiac myocyte of wildtype embryos at 36 hpf (hours post fertilization), thick and thin filaments are assembled into nascent myofibrillar arrays (Fig. 3a). At 36 hpf, such arrays can also be found in *pik* mutant embryos, although they are rare (Fig. 3b). By 48 hpf, wildtype cardiac myocytes also have long-range sarcomeres, but no such arrays are ever noted in *pik* mutant heart cells (Fig. 3c,d). This failure to generate normal sarcomeres probably underlies the inability of the *pik* heart to generate significant systolic force.

The other manifestation of the *pik* mutation is the thinness of the cardiac myocytes. In principle, this could be due to cell-autonomous defects related to the absence of Titin, such as failure to generate higher-order sarcomeres. Alternatively, it could reflect non-autonomous regulation. For example, systolic pressure regulates cellular hypertrophy in the mature heart, and systolic pressures are very low in *pik* mutant embryos. Cell-cell signaling also might be perturbed¹⁴. To examine the cell autonomy of the cardiac thinning defect, we carried out transplantation between wildtype and *pik* embryos to generate mosaic hearts composed of wildtype and mutant cells. Labeled *pik* cells survived in wildtype hearts (Fig. 4a), and labeled wildtype cells survived in *pik* mutant hearts (Fig. 4b). In both cases, the cells retained the cellular characteristics of the donor. Thus, wildtype

cells are plump and visually more contractile than mutant cells, even in *pik* hearts, and do not seem to affect the size of neighboring unlabeled mutant cells. In addition, *pik* mutant cells remain thin, even when surrounded by wildtype cells in a wildtype host. In fact, they are poorly contractile and bulge discoordinately outward with each systolic contraction of the wildtype heart, forming single cell aneurysms (Fig. 4c,d). Thus, the *ttn* mutation causes cellular thinning in a cell-autonomous fashion. Given the important role of Titin in generating the passive elastic recoil of the heart¹⁵, it seems likely that lack of Titin also might make the cells less stiff. This would contribute to the propensity of isolated *pik* cells to bulge outward when integrated into a wildtype heart, where chamber pressures are higher than they are in the heart of a *pik* mutant embryo.

The *pik* mutation clearly indicates a requirement for Titin in establishing the earliest embryonic function of the vertebrate heart. The failure to generate higher-order sarcomeric assembly is consistent with the diminution in sarcomerogenesis noted in myofibroblast lines bearing a deletion within *titin*¹⁶ and of adult rat cardiomyocytes exposed to *titin* antisense oligonucleotides¹⁷, and with the effects of mutations at the *D-titin* locus, a *Drosophila* gene orthologous to vertebrate *titin*¹⁸. Three extensible domains within the Titin I-band (Ig-like, PEVK and N2B) provide the spring-like elastic recoil essential to diastolic force^{19,20}. It is thus not unexpected that in the absence of *titin* there is little recoil, so that transplanted *pik* cells bulge outward in wildtype hearts.

The thin-walled, dilated, poorly contractile heart of *pik* embryos resembles those of people with dilated cardiomyopathy, a disease that is often lethal and of unknown cause. It has been suggested, however, that there is a strong genetic contribution to 35% of all cases²¹. In only rare instances have the

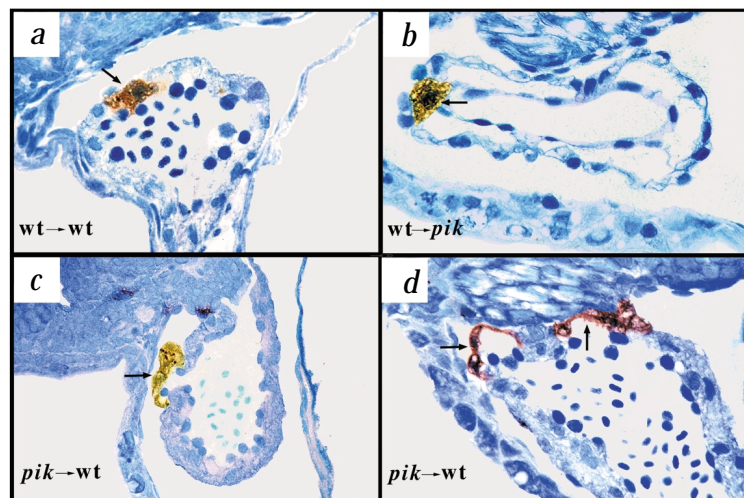


Fig. 4 Cell-autonomous effect of *pik* in the heart. Mosaic hearts are generated by blastomere transplantation and analyzed at 48 hpf. In each case, transplanted cells are brown (biotin-labeled) and indicated by arrows. Longitudinal sections of the ventricle are shown. **a**, Wildtype cells are indistinguishable from the wildtype host. **b**, Cells in a *pik* mutant heart maintain their plump and rounded shape, compared with the elongated and thin cardiomyocytes of the *pik* mutant. They often seem to better approximate the endocardium than do mutant cells, but it is not clear if this is owing to their contraction or local adhesion. **c,d**, *pik* cells in wildtype hearts are thin and bulge outwards.

responsible mutations been identified. These are in genes encoding dystrophin²², β -myosin²³, actin²⁴ and lamin²⁵. The gene *ttn* is at a locus orthologous to one associated with human dilated cardiomyopathy; a related study⁸ in this issue describes mutations in *TTN* in families with dilated cardiomyopathy.

Methods

Positional cloning of *pickwick* locus. We established linkage using simple sequence-length polymorphism markers (SSLPs)²⁶. We cloned YAC ends by plasmid rescue. We extracted BAC DNA using a QIAGEN plasmid Midi kit and determined the end sequences by direct sequencing. EST clones were generated by the Washington University zebrafish EST project and purchased from Research Genetics. We determined the physical map of the YAC and BAC clones, using primer pairs derived from the end sequences in standard PCR reactions, and identified SSCP marker B9F2 (Fig. 1) from BAC6 *Bam*HI-digestion products. We tested single-strand conformation polymorphisms (SSCPs) on 6% MDE acrylamide (FMC Bioproducts) gels.

Cloning of the zebrafish N2B domain and identification of point mutation. We extracted mRNA from pools of ten adult zebrafish hearts using TRIzol reagent (GibcoBRL). We amplified the adult zebrafish *ttn* N2B exon using the Expand 20 kbPlus PCR System (Roche), cloned the 4.6-kb PCR product using a TOPO TA Cloning Kit (Invitrogen) and determined the sequence using EZ:TN <TET-1> Insertion Kit (Epicentre Technologies). We generated a contig with approximately threefold sequence coverage using Phred/Phrad software. The translated peptide can be read through and is highly homologous to human N2B domain.

We then cloned the N2B exons from different *pik* alleles using three overlapping primer pairs. We isolated and reverse transcribed cDNAs from pools of ten zebrafish homozygous mutant embryos at two days post fertilization (dpf) to generate templates. We compared the sequences using a MutationScreener Kit (Ambion) and detected a mismatch between products from *pik^{m171/m171}* and wildtype embryos. We sequenced the PCR products and identified a T→G transversion in the cDNA from homozygous *pik^{m171/m171}* embryos. We confirmed the mutation in genomic sequence from *pik^{m171/m171}* embryos. PCR primer sequences are available from the corresponding author upon request.

In situ hybridization. We carried out whole-mount *in situ* hybridization as described²⁷. We generated the RB1 probe (Fig. 2) from a PCR product using T7 promoter tagged primer pairs. We generated probe RB2 by digesting the EST clone AI629069 (Research Genetics) with *Sal*I.

Morpholinos. We purchased morpholino antisense oligonucleotides from Gene Tools. We prepared and injected solutions as described²⁸. The sequences are available upon request.

We monitored the splicing events using quantitative RT-PCR (Ambion). The templates were reverse-transcribed cDNAs from pools of roughly 50 embryos at 2 dpf. We determined the linear range of PCR amplification by measuring the incorporation of [α -³²P] dCTP into PCR products. We used 30 cycles for primer set 1 and 25 cycles for primer sets 2 and 3. We included universal 18S rRNA (primers:competimers ratio of 2:8) as an internal standard to calibrate the amounts of starting template. Sequences of PCR primers are available from the corresponding author upon request.

In vivo blood pressure measurement. We obtained *in vivo* continuous recordings of intraventricular blood pressure in *pik* mutants and healthy siblings at 48 hpf. We slightly anesthetized the embryos with a tricaine solution (50 μ g ml⁻¹) in egg water at 28.5 °C and immobilized them by gentle suction with a holding micropipette fitted to a manual microsyringe driver and a 25- μ l Hamilton syringe (Stoelting). We obtained pressure measurements with a servo-null micropressure system, model 5D (Instrumentation for Physiology and Medicine) as previously reported¹². We placed a glass electrode (5- μ m diameter tip) held by a micromanipulator into the lumen of the ventricle and recorded dynamic pressure outputs on a Narco four-channel chart recorder.

Transmission electron microscopy. We fixed embryos in 2% glutaraldehyde in 0.1 M sodium cacodylate buffer (pH 7.4) for 1 h at room temperature. We then carried out postfixation with 1% osmium tetroxide in 0.1 M

sodium cacodylate buffer for 1 h on ice. After rinsing, we dehydrated embryos in a graded series of ethanol-water solutions and infiltrated them in propylene oxide and resin, followed by immersion overnight in 100% resin on a rotator. Resin polymerization was obtained by incubation at 60 °C for 24 h. We cut ultrathin sections (~100 nm) on a Reichert-Jung microtome ('Ultracut E' model) and stained with 3% uranyl citrate and Reynolds lead citrate. We viewed and photographed samples using a Philips CM10 transmission electron microscope.

Blastomere transplantation. We injected donors at the 1–4-cell stage with 4% biotin-dextran and rhodamine-dextran (Molecular Probes) in 200 mM KCL. At the blastomere stage, we carried out reciprocal transplants (wildtype to *pik*, $n=4$; *pik* to wildtype, $n=5$) as previously described²⁹. (In practice, we carried out transplants among unidentified progeny of *pik^{+/m}* × *pik^{+/m}* crosses. We identified mutant embryos among donors and recipients only later, after the phenotypes become evident.) We embedded live recipients in 3% methyl cellulose to assess contractile function of transplanted cardiac myocytes, using an inverted fluorescent microscope (Zeiss Axioskop). We then processed transplanted specimens for whole-mount staining of co-injected biotin-dextran.

GenBank accession number. *ttn* mRNA, N2B domain, AY033829.

Acknowledgments

We thank M. McKee and D. Brown for transmission electron microscopy services. This work was supported in part by grants from the National Institutes of Health and a sponsored research agreement by Genentech (M.C.F.), the Foundation for Anesthesia Education and Research (S.E.M.) and a Postdoctoral Fellowship of American Heart Association (X.X.).

Received 22 August; accepted 5 December 2001.

- Burggren, W.W. & Pinder, A.W. Ontogeny of cardiovascular and respiratory physiology in lower vertebrates. *Annu. Rev. Physiol.* **53**, 107–135 (1991).
- Driever, W. *et al.* A genetic screen for mutations affecting embryogenesis in zebrafish. *Development* **123**, 37–46 (1996).
- Stainier, D.Y. *et al.* Mutations affecting the formation and function of the cardiovascular system in the zebrafish embryo. *Development* **123**, 285–292 (1996).
- Warren, K.S., Wu, J.C., Pinet, F. & Fishman, M.C. The genetic basis of cardiac function: dissection by zebrafish (*Danio rerio*) screens. *Philos. Trans. R. Soc. Lond. B Biol. Sci.* **355**, 939–944 (2000).
- Labeit, S. & Kolmerer, B. Titins: giant proteins in charge of muscle ultrastructure and elasticity. *Science* **270**, 293–296 (1995).
- Gregorio, C.C., Granzier, H., Sorimachi, H. & Labeit, S. Muscle assembly: a titanic achievement? *Curr. Opin. Cell. Biol.* **11**, 18–25 (1999).
- Granzier, H.L. & Irving, T.C. Passive tension in cardiac muscle: contribution of collagen, titin, microtubules, and intermediate filaments. *Biophys. J.* **68**, 1027–1044 (1995).
- Gerull, B. *et al.* Mutations of *TTN*, encoding the giant muscle filament titin, cause familial dilated cardiomyopathy. *Nature Genet.* **30**, 201–204 (2002).
- Freiburg, A. *et al.* Series of exon-skipping events in the elastic spring region of titin as the structural basis for myofibrillar elastic diversity. *Circ. Res.* **86**, 1114–1121 (2000).
- Draper, B.W., Morcos, P.A. & Kimmel, C.B. Inhibition of zebrafish fgf8 pre-mRNA splicing with morpholino oligos: a quantifiable method for gene knockdown. *Genesis* **30**, 154–156 (2001).
- Weinstein, B.M., Stemple, D.L., Driever, W. & Fishman, M.C. Gridlock, a localized heritable vascular patterning defect in the zebrafish. *Nature Med.* **1**, 1143–1147 (1995).
- Pelster, B. & Burggren, W.W. Disruption of hemoglobin oxygen transport does not impact oxygen-dependent physiological processes in developing embryos of zebra fish (*Danio rerio*). *Circ. Res.* **79**, 358–362 (1996).
- Trinick, J. Titin as a scaffold and spring. *Curr. Biol.* **6**, 258–260 (1996).
- Hertig, C.M., Kubalak, S.W., Wang, Y. & Chien, K.R. Synergistic roles of neuregulin-1 and insulin-like growth factor-I in activation of the phosphatidylinositol 3-kinase pathway and cardiac chamber morphogenesis. *J. Biol. Chem.* **274**, 37362–37369 (1999).
- Cazorla, O. *et al.* Differential expression of cardiac titin isoforms and modulation of cellular stiffness. *Circ. Res.* **86**, 59–67 (2000).
- van Der Ven, P.F., Bartsch, J.W., Gautel, M., Jockusch, H. & Furst, D.O. A functional knock-out of titin results in defective myofibril assembly. *J. Cell. Sci.* **113**, 1405–1414 (2000).
- Person, V., Kostin, S., Suzuki, K., Labeit, S. & Schaper, J. Antisense oligonucleotide experiments elucidate the essential role of titin in sarcomerogenesis in adult rat cardiomyocytes in long-term culture. *J. Cell. Sci.* **113**, 3851–3859 (2000).
- Zhang, Y., Featherstone, D., Davis, W., Rushton, E. & Broadie, K. *Drosophila* D-Titin is required for myoblast fusion and skeletal muscle striation. *J. Cell. Sci.* **113**, 3103–3115 (2000).
- Helmes, M. *et al.* Mechanically driven contour-length adjustment in rat cardiac titin's unique N2B sequence: titin is an adjustable spring. *Circ. Res.* **84**, 1339–1352 (1999).
- Linke, W.A. *et al.* I-band titin in cardiac muscle is a three-element molecular spring and is critical for maintaining thin filament structure. *J. Cell. Biol.* **146**, 631–644 (1999).

21. Grunig, E. *et al.* Frequency and phenotypes of familial dilated cardiomyopathy. *J. Am. Coll. Cardiol.* **31**, 186–194 (1998).
22. Badorff, C. *et al.* Enteroviral protease 2A cleaves dystrophin: evidence of cytoskeletal disruption in an acquired cardiomyopathy. *Nature Med.* **5**, 320–326 (1999).
23. Kamisago, M. *et al.* Mutations in sarcomere protein genes as a cause of dilated cardiomyopathy. *N. Engl. J. Med.* **343**, 1688–1696 (2000).
24. Olson, T.M., Michels, V.V., Thibodeau, S.N., Tai, Y.S. & Keating, M.T. Actin mutations in dilated cardiomyopathy, a heritable form of heart failure. *Science* **280**, 750–752 (1998).
25. Fatkin, D. *et al.* Missense mutations in the rod domain of the lamin A/C gene as causes of dilated cardiomyopathy and conduction-system disease. *N. Engl. J. Med.* **341**, 1715–1724 (1999).
26. Shimoda, N. *et al.* Zebrafish genetic map with 2000 microsatellite markers. *Genomics* **58**, 219–232 (1999).
27. Thisse, C., Thisse, B., Schilling, T.F. & Postlethwait, J.H. Structure of the zebrafish *snail1* gene and its expression in wild-type, spadetail and no tail mutant embryos. *Development* **119**, 1203–1215 (1993).
28. Nasevicius, A. & Ekker, S.C. Effective targeted gene 'knockdown' in zebrafish. *Nature Genet.* **26**, 216–220 (2000).
29. Ho, R.K. & Kane, D.A. Cell-autonomous action of zebrafish *spt-1* mutation in specific mesodermal precursors. *Nature* **348**, 720–730 (1990).

Reproduced with permission of the copyright owner. Further reproduction prohibited without permission.